Multi-modal shear wave de-icing using fibre piezoelectric actuator on composite for aircraft wings

Yu Shi and Yu Jia, *Member, IEEE*

***Abstract*—The formation and accretion of ice on aircraft wings during flight can be potentially disastrous and existing in-flight de-icing methods are either bulky or power consuming. This paper investigates the use of shear wave de-icing driven by a macro fibre piezoelectric composite actuator on a composite plate typically used for aircraft wings. While the few existing research on this novel de-icing approach focused on either theoretical studies or single frequency mode optimisation that required high excitation amplitudes, this study revealed that the use of multi-modal excitation through broadband frequency sweeps has the potential to promote the chance of shear stress induced de-icing at a relatively small excitation amplitude. The results reported here form the foundation for a pathway towards low power and lightweight de-icing mechanism for in-flight aircraft wings.**

***Index Terms*—De-icing, shear wave, piezoelectric, carbon fibre reinforced plastic (CFRP), macro fibre composite (MFC)**

I. Introduction

DE-ICING is of vital importance to prevent a build up of ice on aircraft surfaces such as wings, empennage and fuselage. During flight, low temperature can result in the supercooling and freezing of precipitation and moisture on the composite surface, which if allowed to accumulate, can compromise fuel efficiency [1]. Different types of ice accretion can occur on aircraft wings [2], [3], including: rime ice, glaze ice, residual ice and a mixture of rime or glaze ice.

Rime ice are typically formed from the supercooling of micro-droplets of water molecules and the freezing of which upon immediate impact onto around the leading edge of the aerofoil. These are typically opaque in nature and conforms to the aerofoil shape. On the other hand, glaze or clear ice is formed from macro-droplets that do not immediately freeze upon impact but collect on the wing frame before freezing. Also, glaze ice do not necessarily conform to the shape of the aerofoil and can structurally compromise the aerodynamic efficiency of the wing. Residual ice are generally also clear in nature and is formed from refreezing of water bodies left behind from incomplete deicing. Generally, there is likely to be a mixture of rime and glaze ice, but glaze ice is much more dangerous because of its weight, shape and harder to de-ice due to a larger contact area with the wing surface.

The formation of ice on in-flight aircraft wings (figure 1a), especially glaze ice, is particularly problematic as it would add significant weight, compromise the aerodynamic efficiency, reduce lift force (figure 1b) and promote turbulence [4]. This would in turn increase drag, compromise the aerodynamics of the aerofoil, and even escalate the risk of crash. Around 10% [5] of historic passenger flight accidents can be attributed to the icing of wings, such as the crash of Air Ontario Flight 1363 [6] and American Eagle Flight 4184 [7].

(a) Ice formation. Image courtesy of NASA [8].

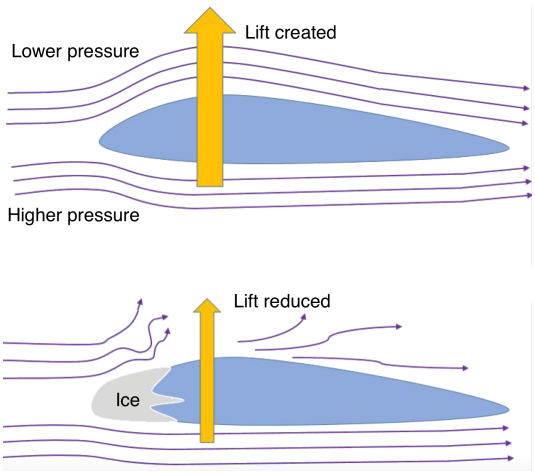

(b) Increase in drag and turbulence [4].

Fig. 1. Ice formation on aircraft wing during flight compromises the lift force and increases risk of accidents as well as reducing fuel economy.

While there have been several advances in ice detection by incorporating sensing methods [2] such as magnetostrictive, electromagnetic and ultrasonic; de-icing methods widely employed still primarily involve chemical and/or heating methods while the airplanes are on the ground in airports [1]. After takeoff, many airplanes primarily rely on a coating of ice suppressant to prevent new ice from forming. In-flight de-icing mechanisms do exist, including: heating systems under

Dr Yu Shi and Dr Yu Jia are with the Department of Mechanical Engineering, Thornton Science Park, University of Chester, Chester, CH2 4NU, UK, (Corresponding author e-mail: yu.jia.gb@ieee.org)

the wings, electrically conductive foil, dispenser systems for antifreeze chemical liquids and mechanical flexing of airplane wings to shake off ice [9], [10].

However, most of these mechanisms are bulky, expensive and power hungry, which are typically suitable only for large aircrafts or military jets. During cold weather conditions, many aeroplanes without in-flight de-icing systems suffer from substantial delays due to the need to complete deicing in the airport; therefore, resulting in non-trivial economic implications. For instance, during the 2016/2017 winter season, Munich Airport de-iced a total of 9,870 aircrafts on the ground across 169 days [11]. Furthermore, a continued trend of year on year increase in the demand of the already strained de-icing capacity at the airport is expected as number of commercial flights increases.

Even in the case of the lightweight foil mechanism used in smaller aircrafts, it consumes a significant portion of the on-board power budget. The increase in payload from the additional power devices and fuel usage would compromise the overall fuel economy as well as have negative financial and environmental impacts. Therefore, there is a gap in developing towards high efficiency, low power and light weight in-flight de-icing methods in order to improve safety, reduce the de-icing demand on certain airports and improve the economic efficiency of operating commercial flights. In particular, considering the streamline design of aircraft structure, the ease of fabrication and integration with existing aerofoil is also a key factor in order to optimise the structural design.

More recently, there are research proposing the use of piezoelectric actuator for de-icing [12], [13], [14], [15], [16]. In general, piezoelectric actuators only require low power consumption to induce vibrations. Moreover, the piezoelectric actuator can be easily integrated within the surface skin to avoid any impact on structural design [17]. The principle of using piezoelectric actuator to remove the ice formed is to deliver shear stress wave excitations. Ice can be released once the shear stresses between the ice and the material surface exceed the adhesive shear strength of the interface (0.24-1.7 MPa [15], [16], [18]). Though, the adhesive properties are dependent on various factors such as temperature, humidity, pressure, wind speed, air density, type of ice, etc [19].

However, most researches reported to date primarily focused on the development of analytical or numerical studies to assess the feasibility of this de-icing method [12], [20], [21], [22], with little successful experimental validation. Aretxabaleta *et. al.* [12] identified the 3rd resonant mode as the one that produced the highest shear stress amongst the first 8 modes through simulation and experiment. However, their experimental de-icing test failed to remove the ice blocks. Furthermore, since the experimental procedure was challenging to control in terms of producing and handling ice, Kalkowski *et. al.* [13] use plaster instead, which has a similar Young's modulus as ice. Though, the adhesion mechanics of plaster is fundamentally different from that of ice.

In addition, it was found for the experiment performed using real ice in a low temperature conditions, in order to remove the ice block, high amplitude input was needed. Although ice was demonstrated to have been successfully removed in some cases, a maximum input voltage of 500 V was applied by Palacios *et. al.* [23] while the signal amplitude of 300 V was selected by Ameduri *et al.* [20]. This, in essence, required the application of high levels of brute shear force that required high power supply.

This research develops a low power and lightweight method of applying the principle of shear wave for the purpose of de-icing on the surface of a composite material typically used on aircraft wing. The macro fibre composite (MFC) piezoelectric actuator was appropriately selected to be easily compatible with fabrication of streamlined composite wing. MFC is lightweight, low power and can be integrated with existing aerospace composite material. This builds onto and extends beyond the previous work by one of the authors in the areas of integration of MFC into aircraft composite [24], as well as the investigation of delamination behaviour of composite materials [25], [26]. Finite element model was explored to study the mechanical vibration modes to find the maximum shear stress generated as references of experimental input. The ice was created while interfacing with the surface of an aircraft composite inside a freezer at realistic temperature conditions when an aircraft is in flight. The same temperature condition was kept consistent during the experiment in order to validate the feasibility of achieving de-icing using the proposed method, and thus establishing the foundation for developing towards a low power and lightweight integrated in-flight shear wave de-icing system.

II. Modelling and Experimental Design

A. Design

The idea of using shear stress wave as the principle for de-icing was primarily inspired from the delamination formation and preogression within composite structures [25], [27]. As the effect of single damage mode (I for tension or II/III for shear) or mixed modes (figure 2), the composite laminate was delaminated between the plies laid up with various fibre orientations.

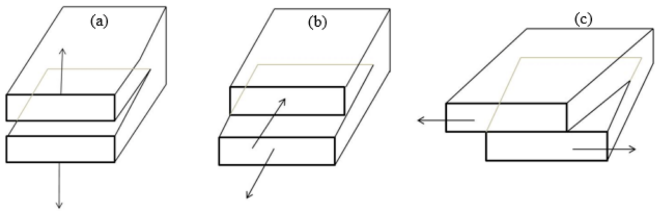

Fig. 2. Three damage modes (a) mode I (opening) (b) mode II (sliding) (c) mode III (tearing).

Therefore, in order to successfully release the ice block formed on the surface of composite wing, the same principle is proposed here. A thin adhesive layer is generally formed between ice and structure surface where the mean tension and shear strengths at this adhesive layers are found to be 300 MPa and 1.65 MPa respectively [28]. Obviously, comparing to the tension strength (mode I), the shear strength of adhesive layers is much smaller and therefore easier to be broken. The shear wave could be delivered to the adhesive layer by exciting the

piezoelectric actuator and the ice block can be removed once the shear stress exceeds the strength of adhesive layer. The schematic of principle using shear stress wave for de-icing is illustrated in figure 3. The transverse shear stress τ_{xz} and τ_{yz} mainly play the roles to get rid of the ice, while in-plane shear stress τ_{xy} contributes to break the ice.

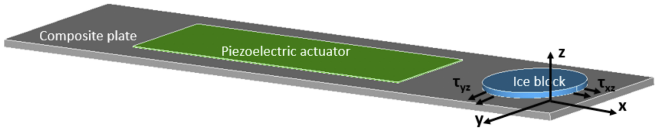

Fig. 3. Schematic of de-icing experiment with shear stress at contact surfaces between ice block and composite plate.

In this work, the aerospace grade carbon fibre/epoxy prepreg T300H/914 was fabricated with size of 175mm × 45mm × 2 mm and designed to lay up with stacking sequences of $[0_2/90/0_2/90/0_2]_S$. Due to the proposed approach is applied for aircraft in flight, the main selection criteria of piezoelectric actuator should be able to work under a low temperature condition (about $-50\,^{\circ}\mathrm{C}$ for heights up to 1500 m [29]) while it is compatible to be integrated with streamlined airframe structures. The macro fibre composite (MFC) offers well flexibility feather resulting from their polymer shell [30] and has been successfully used to the space shuttle missions, which was proven that it could work for environment with low temperature. Therefore, MFC was determined to be piezoelectric actuator to excite the vibration to form shear stress wave. Both key material properties of carbon fibre/epoxy T300/914 and MFC are listed in tables I and II.

TABLE I
MATERIAL PROPERTIES OF THE CARBON FIBRE/EPOXY UNIDIRECTIONAL LAMINATE [31].

Material property	Value
Elastic moduli E (GPa)	$E_1 = 131.9$; $E_1 = 9.51$; $E_1 = 9.43$
Shear moduli G (GPa)	$G_{12} = 5.27$; $G_{13} = 5.27$; $G_{23} = 3.39$
Poisson's ratio ν	$\nu_{12} = 0.326$; $\nu_{13} = 0.341$; $\nu_{23} = 0.485$
$l \times w \times h$ (mm)	175 × 45 × 2

TABLE II
MACRO FIBRE COMPOSITE (MFC) M8525-P2 PROPERTIES [32], [33].

Material property	Value
Mechanical properties	
Elastic modulus E_1 rod direction (GPa)	30.34
Elastic modulus E_2 electrode direction (GPa)	15.86
Shear modulus, G_{12} (GPa)	5.52
Possion's ratio ν_{12}	0.31
$l \times w \times h$ (mm)	85 × 28 × 0.3
Piezoelectric and electrical properties	
Charge constant d_{31} (C/N)	-1.7×10^{-10}
Charge constant d_{33} (C/N)	4.0×10^{-10}
Relative permittivity ϵ_r	1694
Capacitance (F)	1.2×10^{-7}

B. Analytical

For a free vibrating rectangular plate with width b, length l and thickness h, out-of-plane displacement z and in-plane motion along x and y, the total energy of the plate bending system can be expressed as $T+U$ [34]. Where, the total strain potential energy U can be written as shown in equation 1 and the total kinetic energy T can be written as shown in equation 2.

$$U = \frac{k}{2}\int_{-b/2}^{b/2}\int_{-l/2}^{l/2}[(\frac{\delta^2 z}{\delta x^2})^2 + (\frac{\delta^2 z}{\delta y^2})^2 + 2\nu(\frac{\delta^4 z}{\delta x^2 \delta y^2}) + 2(1-\nu)(\frac{\delta^2 z}{\delta x \delta y})^2]\ \mathrm{d}x\ \mathrm{d}y \quad (1)$$

$$T = \frac{\rho h \omega_0^2}{2}\int_{-b/2}^{b/2}\int_{-l/2}^{l/2} z^2\ \mathrm{d}x\ \mathrm{d}y \quad (2)$$

where ν is the Poisson's ratio, ρ is mass density, ω_0 is angular natural frequency and k is the stiffness term defined by equation 3 with elastic modulus E.

$$k = \frac{Eh^3}{12(1-\nu^2)} \quad (3)$$

The average shear stress τ_{av} on the composite material can be approximated by the average shear force $V(y)$ per unit area A of the composite surface: $\tau_{av} = V(y)/A$. During bending, the shear stress can be defined by equation 4.

$$\tau_{yz} = \frac{V(y)}{Ib(z)}\int_z^{z_{max}} zb(z)\ \mathrm{d}z \quad (4)$$

where, τ is the shear stress, V is the shear force, I is the area moment of inertia, b is the width, and y and z are the planar axes on which the shear stress of interest develops.

During the fundamental bending modes, normal stress is typically more prominent than transverse shear stress. However, at higher transverse, lateral and torsional modes, shear stress onsets with a variety of mode shapes at various local points. For some higher resonant modes, shear stress at certain local regions becomes dominant and therefore suitable for breaking the adhesive bonds between ice and the composite surface at these local regions.

The average power consumption P_{av} of a piezoelectric actuator can be estimated by equation 5 [13], [35].

$$P_{av} = \frac{v_s^2}{2}[\frac{Z_L}{(Z_L + Z_S)^2}] \quad (5)$$

where, v_s is the supply voltage, Z_L is the load impedance and Z_S is the supply impedance. Therefore, it would be ideal to operate at low voltage and relatively lower frequency range in order to minimise power consumption. With that said, even for up to megahertz range, the power requirement is still relatively low.

Taking a conservative estimate, up to 10 V used in the following experiment, the power density is calculated to be in the order of 1 kW/m^2 for the given plate area. The actual power density is likely to be lower as the effective area is under-estimated in this calculation, limited by plate size used. Though, this already compares favourably to existing in-flight electrical de-icing systems reported at around 2.2 kW/m^2 to 3.6 kW/m^2 [36]. Furthermore, these existing system values

include load cycling in order to minimise power requirement, whereas the estimate for MFC is for continuous operation.

C. FE Simulation

Solid mechanics FEA model was constructed for the composite rectangular plate in COMSOL Multiphysics and its eignfrequencies analysed at various frequency bands. The four bottom corner points of the plate was constrained in order to simulate the plate dynamics. In COMSOL eignfrequency simulation, amplitude output is arbitrary but relative and figure 4e is the colour bar used to visualise the amplitude of the relative shear stress. The 23 component of the stress tensor was looked at in particular to determine shear stress τ_{yz}. The true stress tensor is defined in equation 6 [37].

$$\sigma = \begin{bmatrix} \sigma_{11} & \sigma_{12} & \sigma_{13} \\ \sigma_{21} & \sigma_{22} & \sigma_{23} \\ \sigma_{31} & \sigma_{32} & \sigma_{33} \end{bmatrix} \equiv \begin{bmatrix} \sigma_x & \tau_{xy} & \tau_{xz} \\ \tau_{yx} & \sigma_y & \tau_{yz} \\ \tau_{zx} & \tau_{zy} & \sigma_z \end{bmatrix} \tag{6}$$

The first 3 modes of resonance of the composite rectangular test plate is shown in figure 4. It can be seen that the first transverse normal mode and the first lateral mode do not yield significant shear stress when compared with the first torsional twist mode. Therefore, amongst the first 3 resonant modes, exciting the 3rd mode would provide a more favourable conditions for shear wave de-icing.

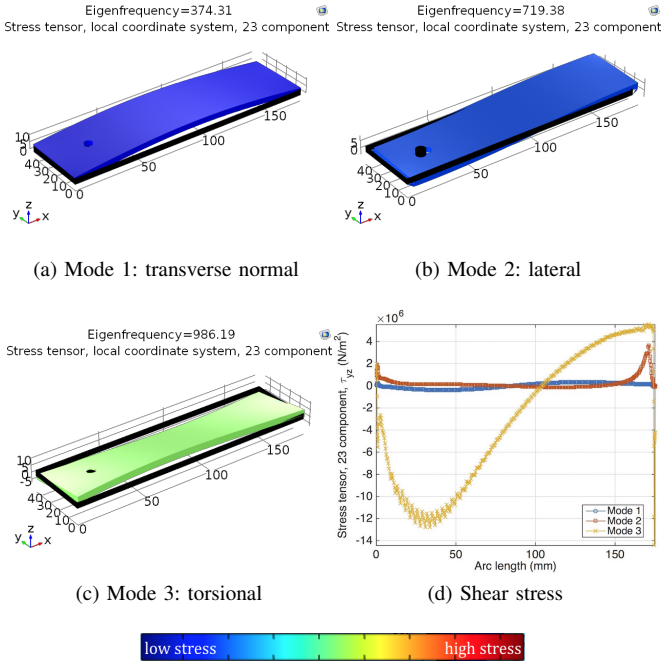

(a) Mode 1: transverse normal (b) Mode 2: lateral

(c) Mode 3: torsional (d) Shear stress

(e) Rainbow colour bar used in this paper

Fig. 4. FEA simulation of the first 3 modes, illustrating their mode shapes and their respective shear stress, 23 component, τ_{yz} along the composite length. The torsional mode has significantly higher shear maxima.

The simulated relative representative values for the average shear stress developed across the composite plate is illustrated in table III. It can be seen that τ_{yz} tend to dominate as the primary source of shear stress in comparison to τ_{xz}. Therefore, in real application, when the amplitude of excitation for these modes reach a level where the anti-nodes of these shear peaks attain the required values to delaminate the ice-composite interface, de-icing at these localised antinodal points can be achieved.

TABLE III
FE SIMULATED SHEAR STRESSES τ_{xz} AND τ_{yz} FOR THE FIRST 6 MODES.

Mode number	Average stress (MPa) τ_{xz}	τ_{yz}	τ_{yz}/τ_{xz}
1	0.16	0.83	5.2
2	0.01	0.12	12.0
3	0.34	1.02	3.0
4	0.15	0.15	1.0
5	0.01	0.01	1.0
6	0.04	0.10	2.5

At higher resonant modes, with the rise of multiple nodal lines along the plate, multiple shear regions can be observed as illustrated in figures 5 and 6. Figure 5 demonstrates the onset of multiple maxima and minima shear stress regions between mode 4 and mode 7. Along the length of composite plate, multiple shear stress peaks (anitnodes) can be observed for higher modes as shown in figure 6.

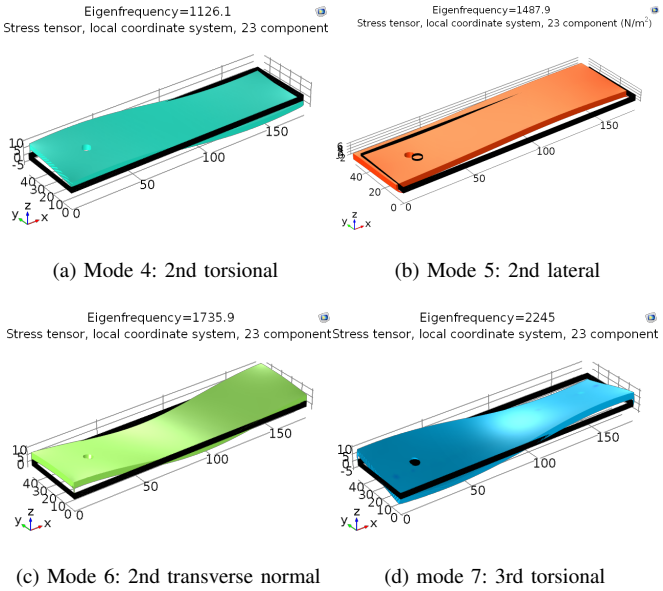

(a) Mode 4: 2nd torsional (b) Mode 5: 2nd lateral

(c) Mode 6: 2nd transverse normal (d) mode 7: 3rd torsional

Fig. 5. FEA simulation of the first few higher modes, showing onset of multiple shear regions, including multiple maxima and minima, due to the increase in nodal lines.

Therefore, shear stress de-icing is potentially more effective at the local regions of shear stress maxima than the minima points. Even for ultra high modes, while there are more numerous numbers of shear stress peaks, there are also equivalent number of nodal points where shear stress is neutral. Therefore, a single resonant mode is effective only for de-icing on specific local regions on the composite surface. For global shear wave de-icing, either multiple resonant modes are required to be activated together or the amplitude of a single shear mode need to be amplified in order to maximise the effect area of that antinode. However, the latter approach is more power consuming. When sufficient number of antinodal points and adequate shear stress amplitudes onset, global

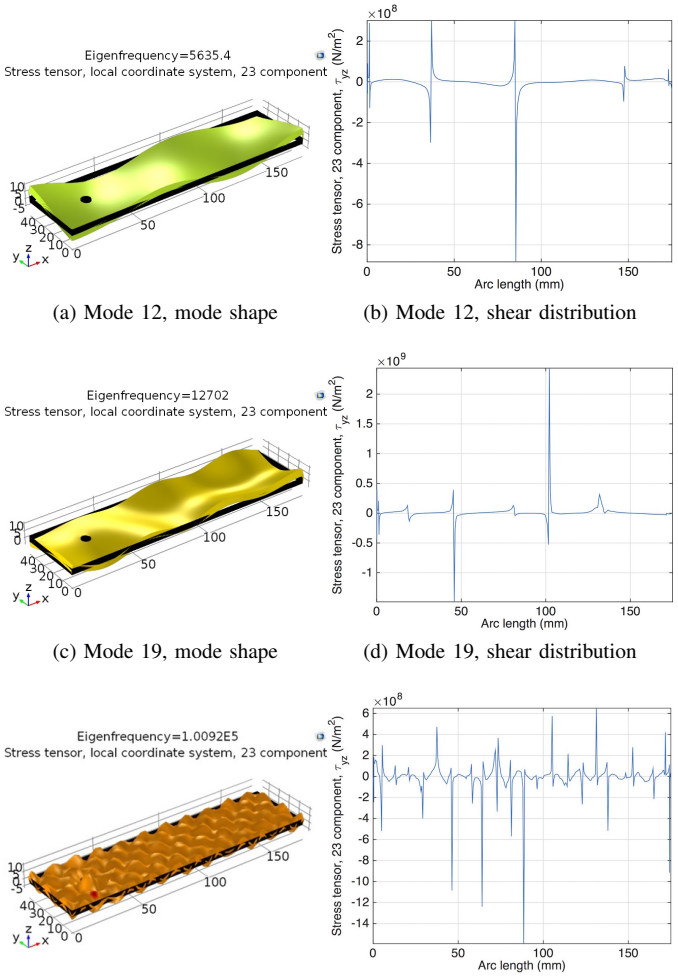

(a) Mode 12, mode shape (b) Mode 12, shear distribution

(c) Mode 19, mode shape (d) Mode 19, shear distribution

(e) Mode 218, mode shape (f) Mode 218, shear distribution

Fig. 6. FEA simulation of selected higher modes, illustrating the distribution of multiple local shear stress regions along the composite length.

delamination of the ice-composite interface can be achieved as shear strength is overcome.

D. Setup and Apparatus

The experiment was carried out to verify the feasibility of de-icing using the proposed shear stress wave method. The experimental setup to produce ice on the composite plate and the experimentation of the de-icing phenomenon is shown in figure 7. The MFC was integrated onto the top surface of composite substrate by Loctite epoxy while the mechanical pressure was applied during the bonding process to minimise the epoxy thickness. A cylindrical measuring tube with inner diameter of 27 mm was used to form the ice block, so that the volume as well as the thickness of the ice block could be accurately determined. A small beaker was used to pour precise volume of water into the measuring tube.

In this work, two volume values of 1.5 ml and 3 ml of ice block were planned aiming to find the optimal efficiency of de-icing with thickness effect. The composite was placed into freezer at $-64\,^{\circ}\mathrm{C}$ for approximately 10 minutes to consolidate the ice. The cylindrical tube was carefully removed through

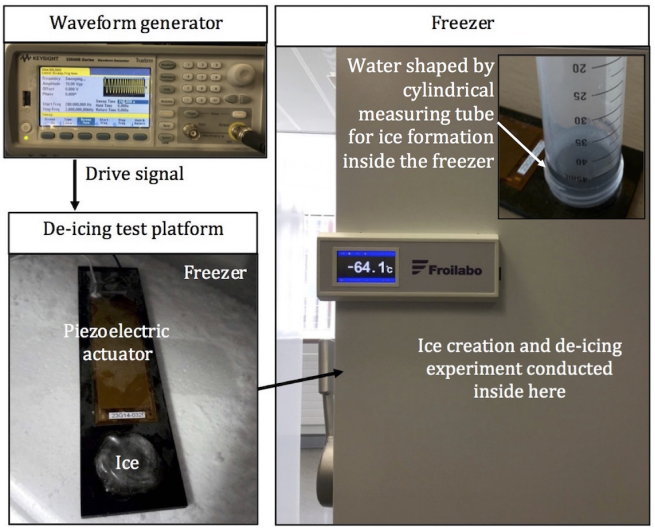

Fig. 7. Experimental apparatus setup. Piezoelectric actuator was bonded to the composite test plate.

twist, prior to the complete consolidation. To excite the mechanical vibration, the MFC was connected with waveform generator which can define the drive signal of the shear stress wave. Based on the FE prediction (figure 4), to maximum the transverse shear stress effect, the 3rd mode with frequency in the vicinity of 990 Hz was set as the initial region of investigation for de-icing with an applied AC voltage capped at 10V peak-to-peak. The excitation amplitude was capped in order to investigate the feasibility of low power de-icing. The experimental temperature was initially consistent with value of $-64\,^{\circ}\mathrm{C}$ because an obvious increasing of temperature was found as the door of freezer was opened during the procedure of experiment. The mean test temperature was maintained around $-60\,^{\circ}\mathrm{C}$, which is in a conservative agreement with the real flight environment conditions [29]. Vibration and shear wave signal will be strongest on the MFC itself, and subsequently weakens further away from the actuator. Therefore, the main ice block is placed on the composite plate right outside the MFC.

III. Results and Discussion

A. Single mode frequency tests

Based on the frequency modes identified in the FE simulation, frequency points for the first few modes of the composite plate were experimentally determined using the technique of Chladni pattern. Piezoelectric transducer was driven by a single frequency sinusoidal signal from a waveform generator and scattered grounded tea powder on the plate surface was used to help determine the experimental frequency points.

This more traditional experimentation method for qualifying and quantifying resonant frequencies and resonant mode shapes were employed due to the lack of access to equipment such as laser doppler vibrometer. Furthermore, while access to electrical measurement techniques such as the use of another sensing transducer and spectrum analyser was available, those indirect measurement methods would not be able to verify the precise mode shapes for a given resonant peak.

The first few modes up to 2 kHz that corresponds to their FEA equivalent, were experimentally recorded as shown in table IV. The frequency of the measured modes were in good agreement with their FEA equivalent, thus giving good confidence for the predicted frequencies for the higher modes that were not measured. Lateral modes were not measurable by the Chladni pattern technique due to the predominantly in-plane vibration at these modes. Furthermore, lateral modes were also not of interest within the scope of this study as outlined in the previous section. The label 'n/m' in the table is used to to denote 'not measured' values.

TABLE IV
FE SIMULATED AND EXPERIMENTALLY MEASURED RESONANT MODES OF THE COMPOSITE PLATE, UP TO 2 KHZ.

Mode number	Frequency (Hz)		Mode type
	Simulation	Experiment	
1	374	∼398	1st transverse normal
2	719	n/m	1st lateral
3	986	∼990	1st torsional
4	1126	∼1182	2nd torsional
5	1488	n/m	2nd lateral
6	1736	∼1920	2nd transverse normal

Table V shows a summary of the various de-icing experiments carried out. Most of the single frequency tests, on 3 ml ice, yielded negative results for excitation amplitude of up to 10 V peak to peak; where the ice block failed to release from the surface. Applying narrow band frequency sweeps around the frequency vicinity of targeted resonant modes, scanning around the 3rd mode between 900 Hz to 1100 Hz revealed the development of some cracks on 3 ml ice after eight 30 s sweeps. However, the ice block as a whole still adhered firmly to the composite surface. There is a possibility that the development of cracks can be further propagated and removed from the surface by the presence of air pressure and macro vibration in the harsh in-flight environment. This result is similar to what was reported by others in the literature that investigated at the 3rd mode in specific [12], [15]; and significantly larger excitation amplitude [15] or significantly long time [23] would be required to de-ice using the 3rd mode.

B. Multi-modal frequency sweep tests

With the presence of nodal points and nodal lines, these are potentially local regions where there is an insufficient amount of shear stress to act against the adhesive bonds of ice to the composite surface. Furthermore, at low temperature of $-60\,^{\circ}\mathrm{C}$, while the other high shear stress local regions are de-iced, the nodal regions can serve as anchors from which the ice would reform its global adhesive bonds. In an attempt to circumvent this, a combination of multiple modes (figure 8) can potentially help to provide shearing to almost all points across the surface area.

This can be practically achieved by either applying a frequency sweep or a periodic chirp across a specific frequency bandwidth, so that multiple modes can be triggered either simultaneous or in close temporal proximity to each other. This would help to onset shear stress at various neighbouring local regions, prior to the ice adhesive bonds retaking hold and

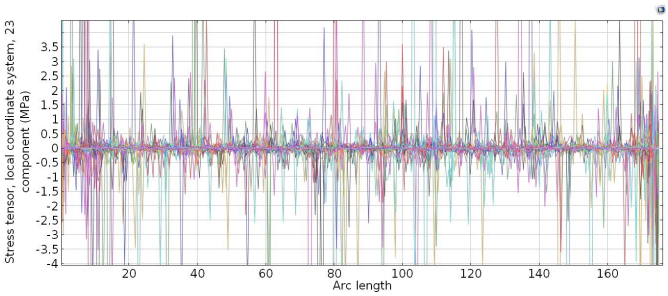

(a) First 250 modes, frequency ranging from 374 Hz to 108.81 kHz

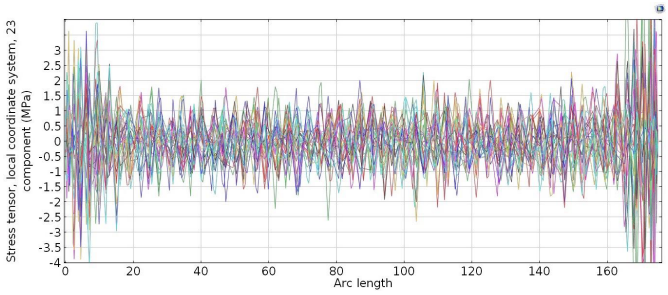

(b) 25 modes around 1 MHz ± 300 Hz

Fig. 8. FEA simulation of overlapping the shear stress distribution of multiple vibrational modes along the composite length.

promote the chance of global de-icing. Also, such broadband approaches would inherently trigger multiple modes and is thus immune to frequency shifts of the mechanical systems. On the other hand, single frequency excitation would need to re-tune the excitation frequency to re-target the intended single resonant mode.

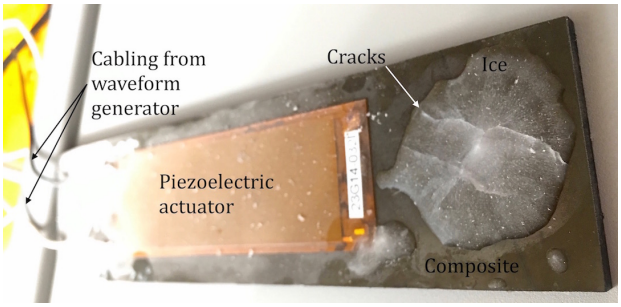

Fig. 9. Experimental result for 1.5 ml frozen water when subjected to broadband frequency sweep. Extensive cracks can be seen to develop after the frequency sweep was applied.

As recorded per table V, selected band sweeps were performed in increments of 100 kHz and 200 kHz, up to 20 MHz. Repeated 240 s sweeps of 3 ml ice did not reveal successful de-icing results for all of the scanned bands. There were no observable signs of crack propagation and the ice remained firmly adhered to the composite surface. This could potentially be because the sweep bandwidth of 100 kHz and 200 kHz were not broadband enough for sufficient multi-modal overlap to accumulate the local shear regions to the proposed global de-icing mechanism.

Broadband frequency sweeps were also carried out, which demonstrated positive de-icing results. 100 Hz to 1 MHz sweep of 1.5 ml ice was able to initiate cracks and eventually

TABLE V
SUMMARY OF VARIOUS EXPERIMENTS UNDERTAKEN. ALL TESTS CARRIED OUT WITH APPARATUS PLACED INSIDE FREEZER AND PIEZOELECTRIC TRANSDUCER DRIVEN BY 10 V PEAK-TO-PEAK SIGNAL FROM THE WAVEFORM GENERATOR.

Experiment description	De-icing success?	Result discussion
Single frequency tests		
1st mode excitation, 3 ml ice, tested up to 10 mins	No	No cracks, ice remains adhered
2nd mode excitation, 3 ml ice, tested up to 10 mins	No	No cracks, ice remains adhered
3rd mode excitation, 3 ml ice, tested up to 10 mins	No	No cracks, ice remains adhered
Up to first 6 modes excitations, 3 ml ice, tested up to 10 mins	No	No cracks, ice remains adhered
Narrow band sweeps		
300 Hz to 600 Hz (targeting 1st mode), 3 ml ice, eight 30 s sweeps	No	No cracks, ice remains adhered
600 Hz to 900 Hz (targeting 2nd mode), 3 ml ice, eight 30 s sweeps	No	No cracks, ice remains adhered
900 Hz to 1100 Hz (targeting 3rd mode), 3 ml ice, eight 30 s sweeps	Semi	Some minor cracks, ice remains adhered
1.1 kHz to 1.3 kHz (targeting 4th mode), 3 ml ice, eight 30 s sweeps	No	No cracks, ice remains adhered
1.4 kHz to 1.8 kHz (targeting 5th mode), 3 ml ice, eight 30 s sweeps	No	No cracks, ice remains adhered
1.8 kHz to 2.0 kHz (targeting 6th mode), 3 ml ice, eight 30 s sweeps	No	No cracks, ice remains adhered
Selected band sweeps		
100 Hz to 100 kHz, 3 ml ice, three 240 s sweep	No	No cracks, ice remains adhered
200 kHz to 300 kHz, 3 ml ice, three 240 s sweep	No	No cracks, ice remains adhered
Further 0.1 MHz increments until 20 MHz, 3 ml ice, three 240 s sweeps	No	No cracks, ice remains adhered
Broadband sweeps, up to megahertz range		
100 Hz to 1 MHz, 1.5 ml irregularly shaped ice, one 100 s sweep	Semi	Some minor cracks, ice remains adhered
100 Hz to 1 MHz, 1.5 ml irregularly shaped ice, five 100 s sweep	Yes	Cracks developed, ice mostly de-bonded
100 kHz to 1 MHz, 3 ml ice, three 100 s sweep	Semi	Some minor cracks, ice remains adhered
100 kHz to 1 MHz, 3 ml ice, three 240 s sweep	Yes	Cracks developed, ice mostly de-bonded
1 MHz to 20 MHz, 3 ml ice, three 240 s sweep	Yes	Cracks developed, ice slid off the surface

loosen the adhesion after a few 100 s sweeps as summarised in table V and captured in figure 9. Both the main ice block and small ice particles on the composite plate were mostly de-bonded and can slide off either with a slight external force or by tilting the composite plate. However, after the removal of shear wave, the residual ice start to re-adhere to the composite surface as expected. In real applications, it is likely that the airflow and wind will be to clear out the de-bonded ice, in order to prevent the residual ice from re-adhering to the surface.

Further tests at 100 kHz to 1 MHz and 1 MHz to 20 MHz sweeps lasting 240 s all revealed positive results as can be seen in table V and figure 10. This suggest that the broader bandwidth of the sweep has activated a large number of resonant modes in quick successions to trigger enough amalgamated local region shear stress that results in global de-icing.

Figure 10a shows the ice on the plate upon ice formation, illustrating firm adhesion to the composite plate. Figure 10b shows the ice disk that has successfully slid off the composite plate surface after the broadband frequency sweeps that has resulted in multi-modal shear wave de-icing. Figure 10c shows cracked segments of circumferential ice left behind after the main ice disk slid off, with a clearly vacated circular surface area at the centre. This demonstrates the evidence for crack propagation and shearing of adhesive bonds between the main ice block and the composite surface.

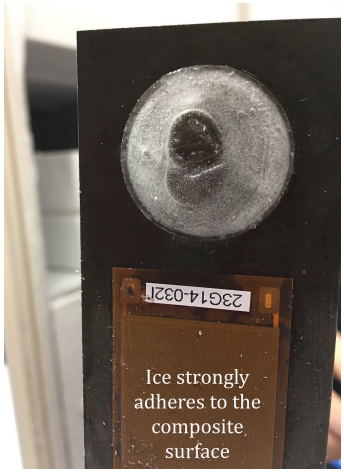

(a) Prior to de-icing

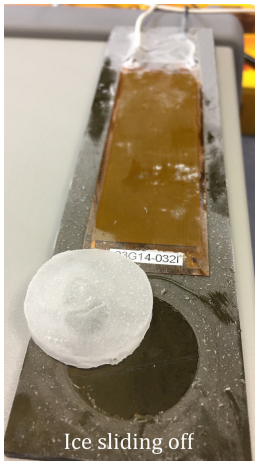

(b) After de-icing

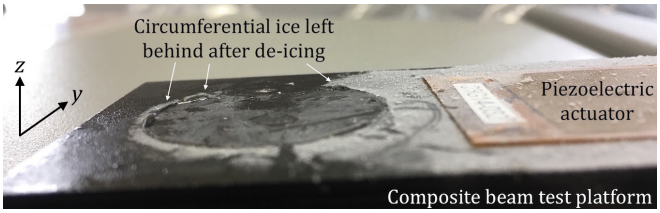

(c) Parts of the circumferential cracked ice left behind after de-icing

Fig. 10. Experimental result for 3 ml frozen water subjected to broadband frequency sweep. De-icing test takes place with the sample inside the freezer in order to avoid influence from ambient heat.

C. Discussion

The various experimental results reported here thus evidence the feasibility of applying shear wave to achieve de-icing through overcoming the shear strength between the ice-composite interface. Broadband sweep induces multiple shear antinodes that is able to help overcome the shear strength at multiple points across the interface contact surface area. Therefore, large amplitude (and power input) to amplify a single shear antinode is not required. However, the effective area and distance from actuator is still limited by shear wave signal from a single MFC. Going beyond the current feasibility

study for localised ice near MFC, multiple MFC arrays would be needed to expand the effective area of the shear wave de-icing to a large area covering the entire aircraft wing.

The substrate sample used in this study is a composite plate typical of the material used on aircraft wing skin. This allows a representative icing interface between the ice and the structure surface. However, the global dynamic structural behaviour would differ to that of a real aircraft wing. Furthermore, airflow, temperature, humidity and pressure conditions for the experiments performed would differ from a representative environment. While the icing temperature of chosen was within the centre range of typical flight environmental conditions [29], real application is likely witness a dynamic temperature profile with time. On the other hand, airflow, pressure and humidity conditions were not possible to match the application environmental conditions within the scope of this study.

IV. Ongoing and future work

Future work will involve parameter optimisation, patterning and orientation of multiple MFC arrays over large area, in order to assess: the shear wave coupling, de-icing efficiency, effective area and develop towards a global de-icing scheme. The collection of real data from aircraft wings is also proposed in order to analysis the performance of shear force de-icing under various airflow, temperature and pressure conditions. Furthermore, possible testing on scaled prototype wing model in wind tunnel will also help to validate the concept in representative conditions.

Based on previous integration experience for another application [24], MFC will also be integrated into the top layer of the the composite during prepreg stage in order to validate the performance of a fully integrated composite stack. Future work will also investigate the possibility to integrate with MEMS frequency controllers [38], macro-scale [39] and MEMS [40], [41] piezoelectric vibration energy harvesting, FPGA, microcontrollers and thin film power electronics, in order to realise a low power, light weight and thin profile smart shear wave de-icing system that can be integrated into the CFRP composite stack.

V. Conclusion

This paper investigated the design, simulation and experimental investigation of the feasibility of employing shear wave driven by a macro fibre piezoelectric transducer as a means of de-icing on composite aircraft wings. Drive signals were intentionally capped at a maximum of 10 V peak to peak in order to explore the possibility of achieving shear wave de-icing with relatively low excitation amplitude. Single frequency shear stress wave targeting single high shear stress modes required relatively high levels of amplitude and lengthy time period to de-ice. On the other hand, the activation of a large number of resonant modes in quick succession through repeated frequency sweeps has been demonstrated as a more efficient method of shear wave de-icing. Various local shear stress regions from the multi-modal shear waves can amalgamate to effective shear stress across the entire surface area and achieve de-icing globally on the composite surface within the effective area. Therefore, shear wave de-icing can thus be achieved with a relatively low excitation amplitude compared to single frequency excitation targeting a single mode. Furthermore, the sweep method is immune to frequency shifts of the mechanical system.

Acknowledgment

This work was supported in part by institutional funding from the HEFCE allocation to the University of Chester.

The authors would like to thank Prof C. Soutis and Mr T. Lucas at the Northwest Composites Centre, University of Manchester, for providing the test composite.

References

[1] P. Greg, "Keeping ice off airplane wings," *Mechancial Engineering*, vol. 119, no. 5, pp. 74–76, 1997.

[2] H. Gao and J. Rose, "Ice detection and classification on an aircraft wing with ultrasonic shear horizontal guided waves," *IEEE Transactions on Ultrasonics, Ferroelectrics, and Frequency Control*, vol. 56, no. 2, pp. 334–344, 2009.

[3] H. Addy Jr, "Ice accretions and icing effects for modern airfoils," United States Department of Transportation Federal Aviation Administration, Tech. Rep. NASA/TP-2000-210031, April 2000.

[4] Marshall Editions Ltd, *The Air Traveler's Handbook: The Complete Guide to Air Travel, Airplanes, and Airports*. St Martins Pr, 1989.

[5] K. Petty and C. Floyd, "A statistical review of aviation airframe icing accidents in the u.s," National Transportation Safety Board, Tech. Rep., 2000.

[6] V. Moshansky, "Commission of inquiry into the air ontario crash at dryden, ontario," Commission of Inquiry - Canada, Tech. Rep., March 1992.

[7] National Transportation Safety Board, "Aircraft accident report: In-flight icing encounter and loss of control simmons airlines, d.b.a. american eagle flight 4184," National Tehcnical Information Service, Roselawn, Indiana, Tech. Rep., 1994.

[8] NASA. (2015) NASA, canadian agency renew agreement to reduce aviation icing risks. [Online]. Available: https://www.nasa.gov/sites/default/files/thumbnails/image/15-097.jpg

[9] J. Laforte, M. Allaire, and J. Laflamme, "State-of-the-art on power line de-icing," *Atmospheric Research*, vol. 46, no. 1-2, pp. 143–158, 1998.

[10] G. Isaac, S. Cober, J. Strapp, A. Korolev, A. Tremblay, and D. Marcotte, "Recent canadian research on aircraft in-flight icing," *Canadian Aeronautics and Space Journal*, vol. 47, no. 3, pp. 1–9, 2001.

[11] Aircraft deicing towing pushback, "Report on the de-icing season 2016/2017 at munich airport," Aircraft de-icing and towing services Munich Airport, Tech. Rep., 2016.

[12] L. Aretxabaleta, M. Mateos, J. Abete, and A. Aizpuru, "De-icing of carbon composite platesby piezoelectric actuators," in *15th European conference on composite materails*, Venice, Italy, 24-28 June 2012.

[13] M. K. Kalkowski, T. P. Waters, and E. Rustighi, "Removing surface accretions with piezo-excited high-frequency structural waves," *Active and Passive Smart Structures and Integrated Systems 2015*, vol. 9431, p. 94311T, Apr 2015.

[14] J. Nömm, "De-icing of wind turbines with ultrasonic vibrations," Master's thesis, Luleå University of Technology, SE-971 87 LULEÅ Sweden, 2016.

[15] W. Wang and Z. Yang, "Asymmetric temperature load method for simulation study of wing leading edge in flight deicing with mfc," *International Journal of Control and Automation*, vol. 6, no. 6, pp. 359–370, 2013.

[16] S. V. Venna, L. Y., and G. Botura, "Piezoelectric transducer actuated leading edge de-icing with simultaneous shear and impulse forces," *Journal of Aircraft*, vol. 44, no. 2, pp. 510–515, 2007.

[17] Y. Shi, S. Hallett, and M. Zhu, "Energy harvesting behaviour for aircraft composite structures using macro-fibre composite: Part i – integration and experiment," *Composite Structures*, 2016.

[18] S. Ramanathan, V. V. Varadhan, and V. K. Varadhan, "De-icing of helicopter blades using piezoelectric actuators," in *Smart Structures and Materials 2000: Smart Electronics and MEMS*, vol. 3990, 2000, pp. 354–363.

[19] A. Kraj and L. Bibeau, "Measurement method and results of ice adhesion force on the curved surface of a wind turbine blade," *Renewable Energy*, vol. 35, pp. 741–746, 2010.
[20] S. Ameduri, A. Brindisi, and D. Guida, "Investigations on the use of lamb waves for de-icing purposes," in *25nd International Conference on Adaptive Structures and Technologies*, The Hague, The Netherlands, 6-8 October 2014.
[21] C. Yin, Z. Zhang, Z. Wang, and H. Guo, "Numerical simulation and experimental validation of ultrasonic de-icing system for wind turbine blade," *Applied Acoustics*, vol. 114, pp. 19 – 26, 2016.
[22] A. D. Degtyar and S. I. Rokhlin, *Stress Effect on Ultrasonic Wave Propagation Through the Solid-Solid and Liquid-Solid Plane Interface*. Boston, MA: Springer US, 1997, pp. 1699–1706.
[23] J. Palacios, E. Smith, J. Rose, and R. Royer, "Instantaneous de-icing of freezer ice via ultrasonic actuation," *AIAA Journal*, vol. 49, no. 6, pp. 1158–1167, 2016/11/26 2011.
[24] Y. Shi., S. Hallett., and M. Zhu., "Energy harvesting behaviour for aircraft composite structures using macro-fibre composite: Part i - integration and experiment," *Composite Structures*, vol. 160, pp. 1279–1286, 2017.
[25] Y. Shi, T. Swait, and C. Soutis., "Modelling damage evolution in composite laminates subjected to low velocity impact," *Composite Structures*, vol. 94, no. 9, pp. 2902–2913, 2012.
[26] Y. Shi and C. Soutis, "Modelling transverse matrix cracking and splitting of cross-ply composite laminates under four point bending," *Theoretical and Applied Fracture Mechanics*, vol. 83, pp. 73–81, 2016.
[27] Y. Shi, C. Pinna, and C. Soutis, "Modelling impact damage in composite laminates: a simulation of intra- and inter-laminar cracking," *Composite Structures*, vol. 114, pp. 10–19, 2014.
[28] S. V. Venna and Y. J. Lin, "Mechatronic development of self-actuating in-flight deicing structures," *IEEE/ASME Transactions on Mechatronics*, vol. 11, no. 5, pp. 585–592, 2006.
[29] IFALPA, "Cold temperature corrections," The international federation of air line pilots' associations, Tech. Rep., 2014.
[30] B. Williams, B. Grimsley, D. Inman, and W. Wilkie, "Manufacturing and mechanics-based characterization of macro fiber composite actuators," in *Proceedings of the ASME International Mechanical Engineering Conference and Exposition*, New Orleans, Louisiana, 2002.
[31] A. Bezazi, F. Scarpa, and W. Boukharouba, "Mechanical properties of auxetic carbon/epoxy composites: static and cyclic fatigue behaviour," *Physica Status Solidi B*, vol. 246, pp. 2102–2110, 2009.
[32] Smart material. Macro fiber composite - mfc. [Online]. Available: http://www.smart-material.com/MFC-product-main.html
[33] M. Trinadade and A. Benjeddou, "Characterisation of electric field dependence of d31piezolectric macro fibre composites effective properties," in *6th ECCOMAS Conference on Smart Structures and Materials*, Turin, 2013.
[34] A. G. Piersol and T. L. Paez, *Shock and Vibrations Handbook*, 6th ed. McGraw Hill, 2009.
[35] M. Kalkowski, T. Waters, and E. Rustighi, "Delamination of surface accretions with structural waves: piezo-actuation and power requirements," *Journal of Intelligent Materials Systems and Structures*, vol. 28, no. 11, pp. 1–20, 2016.
[36] O. Meier and D. Scholz, "A handbook method for the estimation of power requirements for electrical de-icing systems," in *DLRK*, Hamburg, 31 August - 02 September 2010.
[37] F. Irgens, *Continuum Mehanics*. Springer-Verlag Berlin Heidelberg, 2008.
[38] C. Nguyen, "Mems technology for timing and frequency control," *IEEE transactions on ultrasonics, ferroelectrics, and frequency control*, vol. 54, no. 2, pp. 251–270, 2007.
[39] Z. Yang and J. Zu, "Toward harvesting vibration energy from multiple directions by a nonlinear compressive-mode piezoelectric transducer," *IEEE/ASME Transactions on Mechatronics*, vol. 21, no. 3, pp. 1787–1791, June 2016.
[40] Y. Jia, J. Yan, K. Soga, and A. Seshia, "Multi-frequency operation of a mems vibration energy harvester by accessing five orders of parametric resonance," in *J. Phys. Conf. Ser.*, ser. 1, vol. 476, 2013, pp. pp. 607–611.
[41] Y. Jia and A. A. Seshia, "Power optimization by mass tuning for mems piezoelectric cantilever vibration energy harvesting," *J. MEMS*, vol. 25, no. 1, pp. 108 – 117, 2015.

Dr Yu Shi is currently a Senior Lecturer at the Department of Mechanical Engineering, University of Chester and leads the Advanced Composite Research Group. He has research interests and experience in simulation and non-destructive damage investigation of composites, lamb wave propagation in composites, and integration of composites for energy harvesting. He graduated PhD from the University of Sheffield and then joined the Energy Harvesting group at the University of Exeter as a research fellow. Following that, he worked for Advanced Forming Research Centre (AFRC) to model metal work piece forming/forging process for project from Rolls Royce.

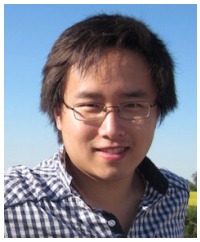

Dr Yu Jia is currently a Senior Lecturer in Mechanical Engineering at the University of Chester and leads the Smart Microsystems Research Group. He is a co-founder of 8power Ltd and a steering board member of the Energy Harvesting Network. He received a First Class (Hon.) in MEng Electromechanical Engineering from the University of Southampton in 2010 and PhD in Engineering from the University of Cambridge in 2014. He was then a Research Associate at Cambridge for a year. His research interests include vibration energy harvesting, micro-electromechanical systems, nonlinear vibration dynamics and smart integrated systems.